FEBS Open Bio 5 (2015) 535–541

FEBS openbio

journal homepage: www.elsevier.com/locate/febsopenbio

2D DIGE proteomic analysis highlights delayed postnatal repression of α-fetoprotein expression in homocystinuria model mice

Shotaro Kamata [a], Noriyuki Akahoshi [b], Isao Ishii [a,*]

[a] Department of Biochemistry, Keio University Graduate School of Pharmaceutical Sciences, Tokyo 105-8512, Japan
[b] Department of Immunology, Akita University Graduate School of Medicine, Akita 010-8543, Japan

ARTICLE INFO

Article history:
Received 14 April 2015
Revised 16 May 2015
Accepted 19 June 2015

Keywords:
α-Fetoprotein
Cystathionine β-synthase
MALDI-TOF/MS
Proteomics
Transcriptional regulation
2D DIGE

ABSTRACT

Cystathionine β-synthase-deficient (*Cbs*$^{-/-}$) mice, an animal model for homocystinuria, exhibit hepatic steatosis and juvenile semilethality via as yet unknown mechanisms. The plasma protein profile of *Cbs*$^{-/-}$ mice was investigated by proteomic analysis using two-dimensional difference gel electrophoresis and matrix-assisted laser desorption/ionization-time of flight/mass spectrometry. We found hyperaccumulation of α-fetoprotein (AFP) and downregulation of most other plasma proteins. AFP was highly expressed in fetal liver, but its expression declined dramatically via transcriptional repression after birth in both wild-type and *Cbs*$^{-/-}$ mice. However, the repression was delayed in *Cbs*$^{-/-}$ mice, causing high postnatal AFP levels, which may relate to transcriptional repression of most plasma proteins originating from liver and the observed hepatic dysfunction.

© 2015 The Authors. Published by Elsevier B.V. on behalf of the Federation of European Biochemical Societies. This is an open access article under the CC BY-NC-ND license (http://creativecommons.org/licenses/by-nc-nd/4.0/).

1. Introduction

Elevated levels of plasma homocysteine are an independent risk factor for atherosclerotic cardiovascular diseases, stroke, peripheral arterial occlusive diseases, and venous thrombosis [1]. Hyperhomocysteinemia is caused by several genetic defects, but mainly by deficiency of cystathionine β-synthase (CBS; EC 4.2.1.22). CBS-deficient homocystinuria patients (MIM 236200) exhibit various severe clinical manifestations including thromboembolism, mental retardation, osteoporosis, and skeletal abnormalities. The molecular mechanisms by which accumulated homocysteine may promote such diseases have been the focus of numerous investigations. Endothelial dysfunction appears to play a key role in cardiovascular diseases [2], but the pathogenesis of hepatic steatosis, a sporadic feature in CBS-deficient patients [1,3], remains to be clarified. It is notable that plasma homocysteine levels are elevated in patients with non-alcoholic fatty liver disease (NAFLD) [4].

A genetic model with targeted deletion of the *Cbs* gene was generated in 1995 [5] and has subsequently been widely used in homocysteine-related research. Homozygous *Cbs*$^{-/-}$ mice develop fatty liver at a juvenile age (~2 weeks old) [5,6] and display an abnormal lipoprotein profile [7], but a few escape and fortunately survive beyond this age [8]. This study examined the plasma protein profile of *Cbs*$^{-/-}$ mice using proteomic analysis with fluorescent two-dimensional difference gel electrophoresis (2D DIGE) to gain insight into the molecular background of hepatic steatosis. For comparison, we utilized mice lacking cystathionine γ-lyase (CTH, also known as CSE; EC 4.4.1.1), which also display homocysteinemia but are free of obvious abnormalities (such as fatty liver) [9]. Here, we found hyperaccumulation of α-fetoprotein (AFP) in the plasma and fatty liver of *Cbs*$^{-/-}$ mice but not of *Cth*$^{-/-}$ mice.

2. Materials and methods

2.1. Animals

Heterozygous *Cbs*$^{+/-}$ mice in a C57BL/6J background (B6.129P2-*Cbs*^{tm1Unc}/J) were obtained from the Jackson Laboratory

Abbreviations: AFP, α-fetoprotein; CBS, cystathionine β-synthase; CTH, cystathionine γ-lyase; DTT, dithiothreitol; HCC, hepatocellular carcinoma; IEF, isoelectric focusing; IPG, immobilized pH gradient; MALDI-TOF/MS, matrix-assisted laser desorption/ionization-time of flight/mass spectrometry; NAFLD, non-alcoholic fatty liver disease; PAGE, polyacrylamide gel electrophoresis; qPCR, quantitative polymerase chain reaction; 2D DIGE, two-dimensional difference gel electrophoresis

* Corresponding author at: Department of Biochemistry, Keio University Graduate School of Pharmaceutical Sciences, Shibakoen 1-5-30, Minato-ku, Tokyo 105-8512, Japan. Fax: +81 3 5400 2671.
E-mail address: isao-ishii@umin.ac.jp (I. Ishii).

http://dx.doi.org/10.1016/j.fob.2015.06.008
2211-5463/© 2015 The Authors. Published by Elsevier B.V. on behalf of the Federation of European Biochemical Societies.
This is an open access article under the CC BY-NC-ND license (http://creativecommons.org/licenses/by-nc-nd/4.0/).

(Bar Harbor, ME, USA). They were further backcrossed for 12 generations (N12) with C57BL/6JJcl (Jcl: Japan Clea, Tokyo, Japan) [8]. Heterozygous $Cth^{+/-}$ mice were generated by our group [9] and backcrossed for 10 generations (N10) with C57BL/6JJcl [10]. N12 $Cbs^{+/-}$ or N10 $Cth^{+/-}$ mice were bred to produce $Cbs^{-/-}$ or $Cth^{-/-}$ mice, and their age-matched progenies were analyzed comparatively. Mice were housed in an air-conditioned room kept on a 12-h dark/light cycle and allowed to free access to a standard dry rodent diet and water. All animal protocols were approved by the Animal Care Committee of Keio University (No. 09187-(4)).

2.2. Polyacrylamide gel electrophoresis (PAGE) and western blotting

Male mice were anesthetized with diethyl ether, and blood samples were collected from beating hearts of laparotomized mice, and then EDTA plasma (or serum) was prepared. Livers were removed quickly and frozen in liquid nitrogen until homogenization in ice-cold phosphate buffer containing Complete Mini, EDTA-free protease inhibitor cocktail (Roche Applied Science) [11]. Serum or liver homogenates (2.5 μg; quantified using Pierce BCA Protein Assay Kit, Thermo Scientific) were separated on a 10% SDS–PAGE gel and transferred to a polyvinylidene fluoride membrane (Immobilon-P, 0.45 μm, Millipore). The membranes were subjected to Western blotting analysis using goat anti-AFP antibody (1:200 dilution; sc-8108; Santa Cruz), anti-glyceraldehyde-3-phosphate dehydrogenase (GAPDH) antibody (1:1,000 dilution; #2118; Cell Signaling), horseradish peroxidase-conjugated anti-goat IgG (H+L) antibody (1:2,000 dilution; PI-9500; Vector Laboratories), and an ECL Prime detection system (GE Healthcare).

2.3. Measurement of plasma albumin levels

Plasma levels of albumin were measured using a Dri-Chem 7000i biochemistry analyzer with ALB-P slides (Fujifilm, Tokyo, Japan).

2.4. 2D DIGE

Plasma (10 μL) was mixed with 90 μL lysis buffer (7 M urea, 2 M thiourea, 4% CHAPS, 1 mM PMSF, 1 mM Na_3VO_4). After adjusting the pH to 8.5 by adding 10 mM Tris–HCl (pH 8.5), 0.8 μL samples were labeled with 200 pmol of CyDye DIGE fluor, minimal labeling dye (Cy2, Cy3 or Cy5 [GE Healthcare]) at 4 °C for 30 min in the dark. The reaction was stopped by adding 0.5 μL of 10 mM lysine. Labeled samples were mixed with dithiothreitol (DTT) and immobilized pH gradient (IPG) buffer (final 1% each) at 4 °C for 10 min in the dark. The samples were immediately subjected to isoelectric focusing (IEF) in an Immobiline DryStrip (13 cm, pH 4–7 [GE Healthcare]) that were rehydrated for 20 h in a rehydration buffer (7 M urea, 2 M thiourea, 2% Triton X-100, 13 mM DTT, 2.5 mM acetic acid, 1% IPG buffer, and a trace amount of bromophenol blue) at 20 °C. IEF was performed using a CoolPhoreStar IPG-IEF Type-PX system (Anatech, Tokyo, Japan) in the following conditions: 500 V for 1.5 h, linear gradient from 500 V to 3500 V for 4.5 h, and finally 3500 V for 8 h at 20 °C. Once IEF was completed, the strips were equilibrated for 30 min in reducing buffer (50 mM Tris–HCl [pH 6.8], 6 M urea, 2% SDS, 30% [v/v] glycerol, 65 mM DTT and a trace amount of bromophenol blue), followed by an alkylating buffer (reducing buffer with 4.5% iodoacetamide instead of DTT) for an additional 15 min. The strips were sealed on the top of 10% PAGE gels using 0.5% low-melting-point agarose in a Tris–glycine electrophoresis buffer. The second dimension of protein separation was performed at a constant 200 V using an ERICA-*S* high-speed electrophoresis system (DRC, Tokyo, Japan) [12]. Gels were scanned using a Typhoon Trio image scanner (GE Healthcare).

2.5. Matrix-assisted laser desorption/ionization-time of flight/mass spectrometry (MALDI-TOF/MS) analysis

For silver staining, plasma (10 μL) was subjected to IEF and then SDS–PAGE without CyDye labeling. The gel was stained using a Silver Stain MS kit (Wako, Tokyo, Japan) in accordance with the manufacturer's instructions. The gel pieces were excised, destained, washed twice with deionized water and four times with 50 mM ammonium bicarbonate: acetonitrile (1:1), and dehydrated once with acetonitrile. Then, the gel pieces were twice alternately rehydrated with 100 mM ammonium bicarbonate and dehydrated with acetonitrile, and dried by vacuum centrifugation. Protein samples were digested at 37 °C for 12 h with 5 μL of 0.02 μg/μL Sequencing Grade Modified Trypsin (Promega) dissolved in 25 mM ammonium bicarbonate. Peptides were extracted from the gels in 40 μL of 1% trifluoroacetic acid/50% acetonitrile solution by sonication. Samples were spotted onto a μFocus MALDI plate (900 μm, 384 circles, Hudson Surface Technology; Old Tappan, NJ, USA) with an equal volume of matrix solution, containing 10 mM α-cyano-4-hydroxycinnamic acid in 1% trifluoroacetic acid/50% acetonitrile. Positive ion mass spectra were obtained using an AXIMA-CFR Plus (Shimadzu, Kyoto, Japan) in a reflectron mode. MS spectra were acquired over a mass range of 700–4000 m/z and calibrated using peptide calibration standards (~1,000–3,200 Da, Bruker Daltonics, Yokohama, Japan) [12].

2.6. Protein database search

Proteins were identified by matching the peptide mass fingerprint with the Swiss-Prot protein database using the MASCOT Search engine (Matrix Science, http://www.matrixscience.com). Database searches were carried out using the following parameters: taxonomy, *Mus musculus*; enzyme, trypsin; and allowing one missed cleavage. Carbamidomethylation was selected as a fixed modification, and the oxidation of methionine was allowed as a variable. The peptide mass tolerance was set at 0.5 Da and the significance threshold was set at $P < 0.05$ probability based values on Mowse scores ($\geqslant 55$).

2.7. Quantitative polymerase chain reaction (qPCR)

Total RNA was isolated from the liver using TRI Reagent (Molecular Research Center, Cincinnati, Ohio, USA). Total RNA (1 μg) was used to produce first-strand cDNA with a ReverTra Ace qPCR RT Kit (Toyobo, Tokyo, Japan). A total of 10 ng of cDNA from each sample was amplified via qPCR using the SYBR Green Realtime PCR Master Mix (Toyobo), 18 primer sets (Table 1), and a CFX96 Touch Real-Time PCR Detection System (Bio-Rad) [11]. Each mRNA level was quantified using the comparative CT method with housekeeping gene *hypoxanthine guanine phosphoribosyl transferase* (*Hprt*) levels used for normalization, and the relative expression in wild-type mice was set at 1.

2.8. Statistical analysis

Data are expressed as means ± SD of independent samples (n as indicated). Statistical analyses were performed using unpaired two-tailed Student's t-test, where P values $\leqslant 0.05$ were considered significant.

3. Results

3.1. Plasma protein profiling by 2D DIGE

$Cbs^{-/-}$ mice suffer from hepatic dysfunction/steatosis [6,7] and start to die from 2 weeks of age, and the majority die by 4 weeks

Table 1
Primer sets for qPCR.

Gene	Primer sequence	Size
Afp	5′-CAGGCACTGTCCAAGCAAAG-3′ (Forward) 5′-ATGAAAATGTCGGCCATTCC-3′ (Reverse)	218 bp
Apoe	5′-TGCTGTTGGTCACATTGCTG-3′ (Forward) 5′-CTGCAGCTCTTCCTGGACCT-3′ (Reverse)	145 bp
Apoa4	5′-AACAATGCCAAGGAGGCTGT-3′ (Forward) 5′-CTGCAGCTCTTCCTGGACCT-3′ (Reverse)	132 bp
A2m	5′-CAGCAGCAGAAGGACAATGG-3′ (Forward) 5′-CAGGCAAAAGAGGGCATTTC-3′ (Reverse)	171 bp
Cp	5′-AGCATTCAGCCAATGGGAGT-3′ (Forward) 5′-GTCCCATTTCTTTGGGGACA-3′ (Reverse)	148 bp
Itih4	5′-CCCGATTTGCCCATACTGTT-3′ (Forward) 5′-CGGCCTTCTCTTTGACAACC-3′ (Reverse)	162 bp
Hpx	5′-ATAGCTGGCCCATTGCTCAT-3′ (Forward) 5′-CTCCAGCCGCTTTGGATAAC-3′ (Reverse)	161 bp
Kng1	5′-CACAGCAACTGTGGGGAAAA-3′ (Forward) 5′-TATGGCATGCACACAACCAA-3′ (Reverse)	124 bp
Serpinc1	5′-AACCGCCTTTTTGGAGACAA-3′ (Forward) 5′-TCTGGATTGCTCCGGATTCT-3′ (Reverse)	120 bp
Serpina1c	5′-TCTTCCTTCTGCCCGATGAT-3′ (Forward) 5′-GTCTGGGGAAGTGGATCTGG-3′ (Reverse)	120 bp
Ahsg	5′-AGATTTCCCGGGCTCAAAAT-3′ (Forward) 5′-GCATGAGATTTGCCTTGCAG-3′ (Reverse)	156 bp
Gc	5′-AGCACTCAGAGTCCCCTGCT-3′ (Forward) 5′-TCCTTAGCCGTTCTGCCAAT-3′ (Reverse)	127 bp
Fgb	5′-CACCTCCATCAAGCCGTACA-3′ (Forward) 5′-TCCCATTTCCTGCCAAAGTC-3′ (Reverse)	111 bp
Fgg	5′-CCTTCTTTGCTGCCTGCTTT-3′ (Forward) 5′-CGTTCGGAGATCATTGTCCA-3′ (Reverse)	172 bp
Apoa1	5′-TGTGTATGTGGATGCGGTCA-3′ (Forward) 5′-ATCCCAGAAGTCCCGAGTCA-3′ (Reverse)	172 bp
Alb	5′-AAAGACGTGTGTTGCCGATG-3′ (Forward) 5′-AGCAGTCAGCCAGTTCACCA-3′ (Reverse)	122 bp
Zbtb20	5′-CCTTCCCTGCCTGAACTTTG-3′ (Forward) 5′-GCACGGAATTGCTGAAGTTG-3′ (Reverse)	176 bp
Hprt	5′-GACTGATTATGGACAGGACTG-3′ (Forward) 5′-GACTGATCATTACAGTAGCTC-3′ (Reverse)	211 bp

[8], and thus we analyzed plasma protein profiles comparatively in 1-, 2-, and 4-week-old $Cbs^{-/-}$ and wild-type mice. Plasma protein concentrations were significantly lower in $Cbs^{-/-}$ mice (24.2 ± 4.5 μg/μL [n = 10] versus 37.2 ± 3.3 μg/μL [n = 8] in wild-type mice at 2 weeks of age; $P < 0.001$), and equal volumes of plasma samples were labeled fluorescently and separated by 2D DIGE (n = 3 for each genotype/age). The obtained fluorescent images indicated that most plasma protein spots were downregulated, whereas only few spots were upregulated in 2-week-old $Cbs^{-/-}$ mice (Fig. 1A), and such changes were not apparent in 1-week-old mice (Fig. 1B) but were generally maintained in 4-week-old mice (Fig. 1C).

MALDI-TOF/MS and Mascot search analyses identified a total of 48 spots for 16 protein species in the plasma samples (Table 2). AFP variants (spots 1a–d) and apolipoprotein E (spot 2) were highly expressed in 2-week-old $Cbs^{-/-}$ mouse plasma, compared with wild-type mouse plasma (Fig. 1A). In contrast, the expression levels of other major plasma proteins, α-2-macroglobulin (spots 4a–f), ceruloplasmin (spots 5a–e), inter α-trypsin inhibitor, heavy chain 4 (spots 6a–d), hemopexin (spots 7a–c), kininogen-1 (spots 8a–d), antithrombin-III (spot 9), α-1-antitrypsin 1-3 (spots 10a–d), α-2-HS-glycoprotein (spots 11a–c), vitamin D-binding protein (spot 12), fibrinogen β chain (spot 13), fibrinogen γ chain (spots 14a–d), and apolipoprotein A-I (spots 15b/c) were significantly downregulated in 2-week-old $Cbs^{-/-}$ mouse plasma (Fig. 1A). Most plasma proteins had several variant spots that dispersed with equal horizontal intervals in IEF; the spots had higher molecular weights as they shifted to lower (acidic) conditions, suggesting that they are redundantly sialylated and thus acidified. Expression of apolipoprotein A-IV (spot 3) and A-I variant (spot 15a) was similar between 2-week-old $Cbs^{-/-}$ and wild-type mouse samples (Fig. 1A), although the expression of both spots increased in 4-week-old $Cbs^{-/-}$ mouse samples (Fig. 1C). The amount of albumin, the most abundant protein in plasma, did not differ significantly (51.1–57.0% [n = 4–6]) among 1-, 2-, and 4-week-old wild-type and $Cbs^{-/-}$ mice (data not shown). Taken together, AFP was enriched whereas most other plasma proteins (except albumin) had decreased levels just before most $Cbs^{-/-}$ mice started to die.

3.2. AFP expression in plasma (serum) and liver

Western blotting analysis using 2D PAGE identified nine AFP-positive spots around 80–90 kDa and pI 5.3–5.8 ranges, and all AFP spots were upregulated in 2-week-old $Cbs^{-/-}$ mouse plasma (Fig. 2A). We next examined AFP expression levels in the serum/liver of 2-week-old wild-type, *Cbs* heterozygous ($Cbs^{+/-}$), $Cbs^{-/-}$, $Cth^{+/-}$, and $Cth^{-/-}$ mice. Serum and hepatic AFP levels were 3.5- and 7.3-fold, respectively, higher in $Cbs^{-/-}$ mice than in wild-type mice (Fig. 2B). AFP expression in $Cth^{-/-}$ mouse serum appeared slightly higher than in wild-type samples, but the difference was not significant (Fig. 2B). We further investigated AFP expression in serum and liver during postnatal development. AFP was highly expressed in embryonic liver and serum, but its expression was repressed postnatally (Fig. 2C). Compared with 2-week-old (P14.5: postnatal day 14.5) wild-type and $Cbs^{+/-}$ mice, in which their hepatic AFP expression was completely repressed and serum AFP expression was mostly repressed, substantial levels of AFP expression were observed in both the liver and serum of 2-week-old $Cbs^{-/-}$ mice (Fig. 2C).

3.3. Transcriptional regulation of plasma proteins

Hepatic mRNA expression of all identified genes was examined by qPCR (Fig. 3). *Afp* expression levels were similar between wild-type and $Cbs^{-/-}$ mice at P0.5. *Afp* expression in wild-type mice decreased dramatically at P14.5 (27.0-fold decrease from P0.5) and P28.5 (1,260-fold decrease), whereas that in $Cbs^{-/-}$ mice increased at P7.5 (2.33-fold increase) and then decreased at P14.5 (2.23-fold decrease) and P28.5 (15.6-fold decrease). As a result, *Afp* expression levels in $Cbs^{-/-}$ mice were 2.16-, 10.2-, and 68.3-fold higher than that in wild-type mice at P7.5, P14.5, and P28.5, respectively. Protein expression of apolipoprotein E was increased (Fig. 1A), but its mRNA expression level was decreased at P14.5 in $Cbs^{-/-}$ mice (Fig. 3). In addition, protein expression of apolipoprotein A-IV was higher in $Cbs^{-/-}$ mice only at P28.5 (Fig. 1C), but its mRNA expression levels were always higher that wild-type mice (Fig. 3). The expression levels of all other genes whose protein expression was significantly lower in $Cbs^{-/-}$ mouse plasma were all decreased in $Cbs^{-/-}$ mouse liver at P14.5 as well as at P28.5, indicating that decreased expression of most plasma proteins is attributable to their reduced mRNA expression in the liver. Xie et al. previously reported that postnatal *Afp* expression in mouse liver is repressed by the zinc finger protein ZBTB20 [13]. Hepatic *Zbtb20* expression was lower in $Cbs^{-/-}$ mice, and therefore, ZBTB20 may be involved in delayed *Afp* repression (Fig. 3).

4. Discussion

AFP is the major serum glycoprotein in the developing mammalian fetus that is produced by endodermal cells of the visceral yolk sac and the liver. The *Afp* gene is highly activated in the fetal liver but dramatically (~10,000-fold) repressed soon after birth, and only trace amounts are detectable in adults [13]. Serum AFP elevation in adults is a well-known marker for hepatocellular

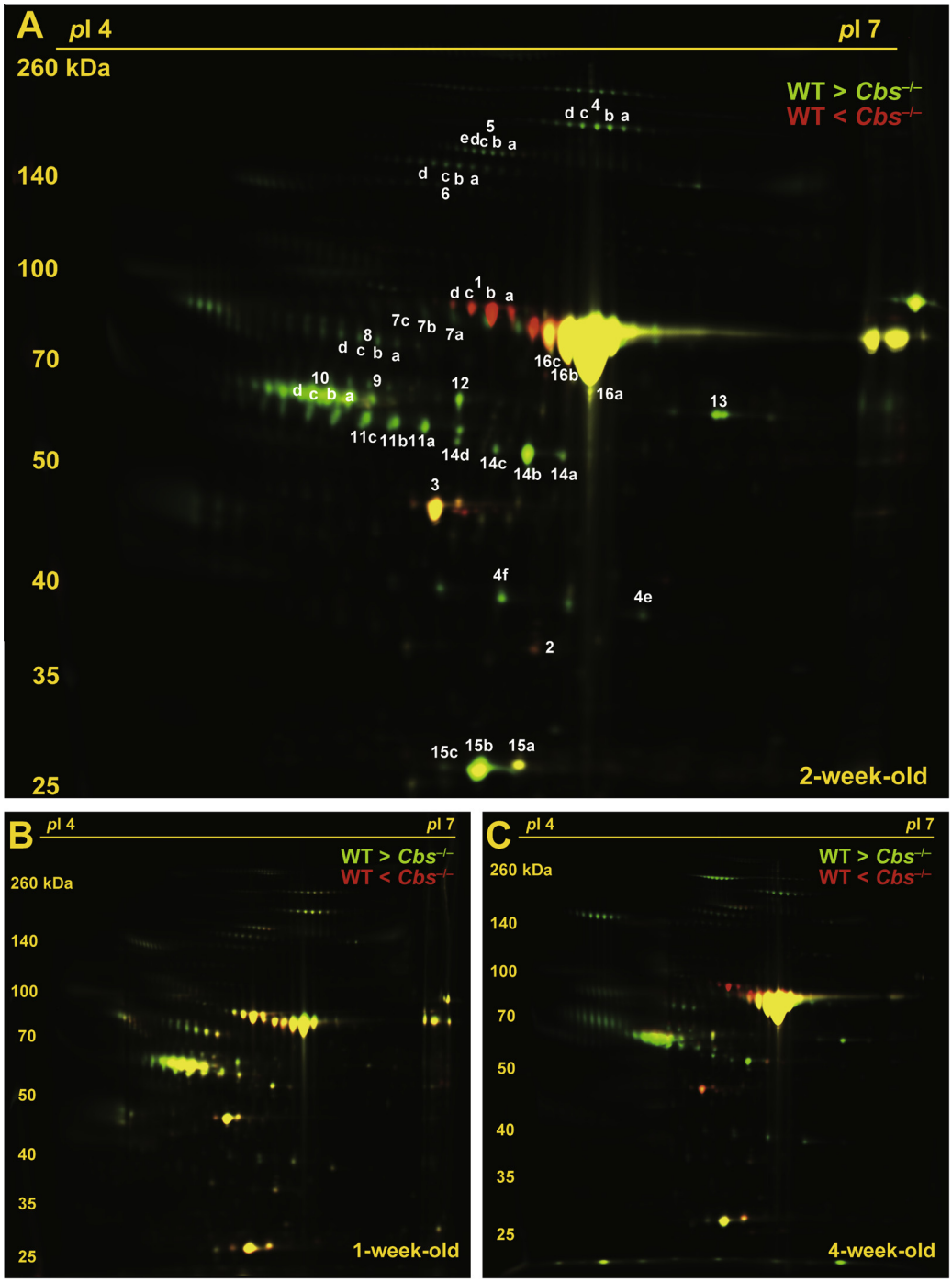

Fig. 1. Altered plasma protein profiles in juvenile *Cbs*$^{-/-}$ mice revealed by 2D DIGE proteomic analysis. Plasma samples from wild-type (WT) and *Cbs*$^{-/-}$ male mice (n = 3 each) at 2 (A), 1 (B), and 4 (C) weeks of age were analyzed comparatively. Representative fluorescent image in which plasma samples from WT and *Cbs*$^{-/-}$ mouse plasma was pseudocolored in green and red, respectively, are presented with approximate isoelectric points (*p*I) and molecular weights (kDa).

carcinoma (HCC), yolk sac tumors, and acute/chronic hepatitis [14,15]. The characteristic machinery of *Afp* repression has attracted considerable attention from researchers interested in transcriptional regulation [13,16,17]; however, despite over 50 years of research since its first discovery in liver cancer, the physiological functions of AFP still remain obscure [14,18]. The main function of AFP is considered to be the extracellular transport of small molecules including estrogens, fatty acids, and bilirubin [19,20], but AFP-deficient mice develop normally and thus AFP is dispensable for embryonic development [21]. Meanwhile AFP is required for fertility in female mice [21] (i.e. protection of the developing female brain from masculinization/defeminization by estrogens [22]) and may play important immune regulatory roles [19,20]. This is the first demonstration of AFP accumulation during juvenile development in CBS-deficient mice, a homocystinuria model that is widely utilized for homocysteine-related research [5–8,12,23]. Our results may be clinically relevant because markedly lower *Cbs* expression in 120 HCC specimens compared with

Table 2
Differentially expressed plasma proteins between 2-week-old wild-type and *Cbs*$^{-/-}$ mice.

Spot ID	Uniprot ID	Unigene	Protein (up or down regulated in *Cbs*$^{-/-}$)	Mascot score	Sequence coverage (%)	Peptide matches	MW_{calc}	pI_{calc}
1 a–d	P02772	*Afp*	α-fetoprotein (up)	218*	64*	36/104*	69,118	5.65
2	P08226	*Apoe*	Apolipoprotein E (up)	172	46	20/36	35,901	5.56
3	P06728	*Apoa4*	Apolipoprotein A-IV (up at 4 weeks)	145	61	23/58	45,001	5.34
4 a–f	Q61838	*A2m*	α-2-macroglobulin (down)	73*	16*	14/39*	167,116	6.24
5 a–e	Q61147	*Cp*	Ceruloplasmin (down)	150*	31*	26/47*	121,872	5.53
6 a–d	A6X935	*Itih4*	Inter α-trypsin inhibitor, heavy chain 4 (down)	100*	30*	25/79*	104,765	5.99
7 a–c	Q91X72	*Hpx*	Hemopexin (down)	115*	42*	18/84*	52,026	7.92
8 a–d	O08677	*Kng1*	Kininogen-1 (down)	112*	26*	18/59*	74,140	6.05
9	P32261	*Serpinc1*	Antithrombin-III (down)	92	35	16/49	52,484	6.10
10 a–d	Q00896	*Serpina1c*	α-1-antitrypsin 1–3 (down)	97*	37*	11/41*	45,966	5.25
11 a–c	P29699	*Ahsg*	α-2-HS-glycoprotein (down)	72*	33*	9/34*	38,100	6.04
12	P21614	*Gc*	Vitamin D-binding protein (down)	121	47	16/61	55,162	5.39
13	Q8K0E8	*Fgb*	Fibrinogen β chain (down)	174	60	35/120	55,402	6.68
14 a–d	Q8VCM7	*Fgg*	Fibrinogen γ chain (down)	212*	71*	24/45*	50,044	5.54
15 a–c	Q00623	*Apoa1*	Apolipoprotein A-I (down)	195*	50*	20/51*	30,597	5.51
16 a–c	P07724	*Alb*	Serum albumin (no change)	263*	60*	31/72*	70,700	5.75

A total 16 proteins identified from MALDI-TOF/MS analysis and Mascot searches are listed with their spot ID (in Fig. 1A), Uniprot ID, Unigene/protein names, Mascot score, sequence coverage, peptide matches, MW_{calc} (molecular weight calculated from identified protein sequence), and pI_{calc} (isoelectric point calculated from identified protein sequence).

* Protein has some variant spots and the representative data from spots with the highest Mascot score are shown.

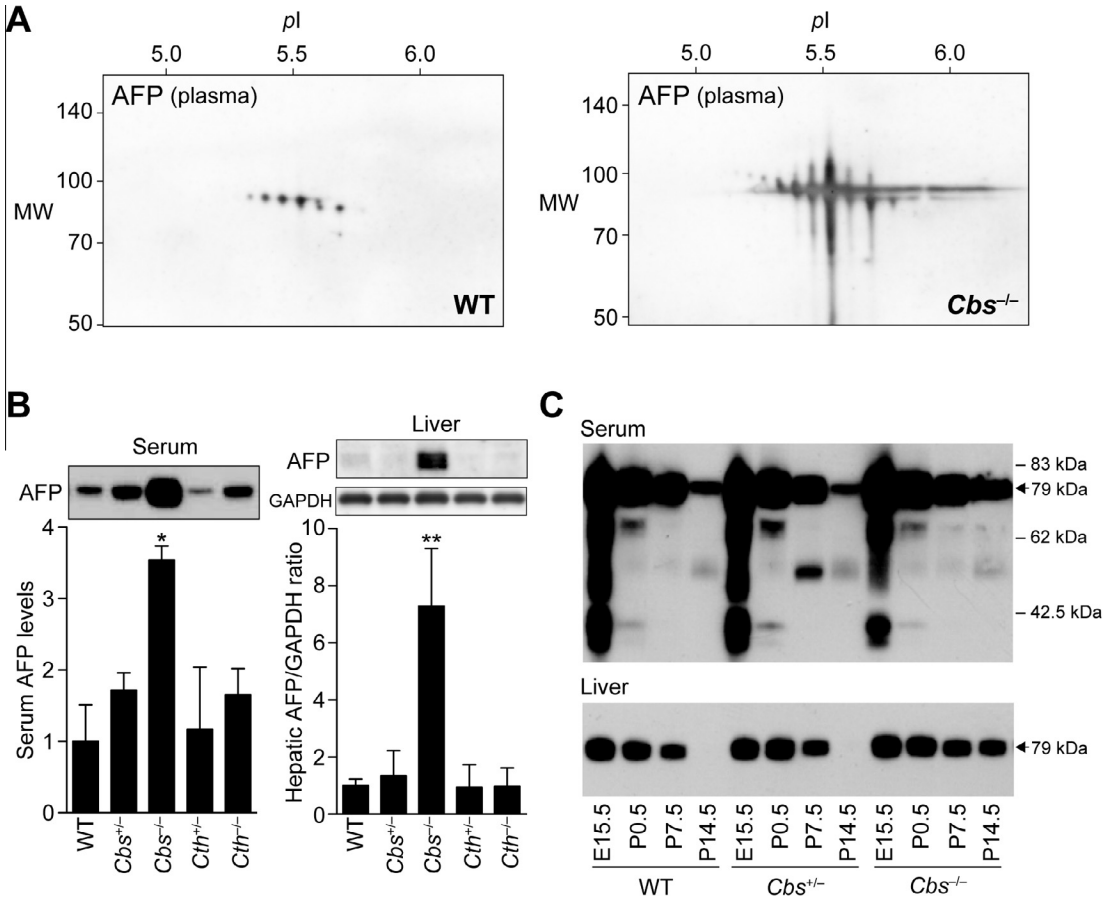

Fig. 2. Increased α-fetoprotein (AFP) expression in 2-week-old *Cbs*$^{-/-}$ mouse plasma/serum/liver. (A) Two-dimensional PAGE/western blotting analysis of AFP variants in 2-week-old wild-type (WT) and *Cbs*$^{-/-}$ male mouse plasma (10 μL). (B) PAGE/western blotting analysis of AFP proteins in 2-week-old WT, (heterozygous) *Cbs*$^{+/-}$, *Cbs*$^{-/-}$, *Cth*$^{+/-}$, and *Cth*$^{-/-}$ mouse serum and liver (2.5 μg protein per lane). As for liver samples, GAPDH expression was examined as a loading control. Band intensities of ~79 kDa AFP proteins were densitometrically scanned and the relative values against the average AFP expression level (for serum) or the AFP/GAPDH ratio (for liver) in WT mouse samples were calculated. The representative band images are presented. Bar data show means ± SD ($n = 3$ each) and differences versus WT are significant at $^{*}P < 0.05$ and $^{**}P < 0.01$ by Student's *t*-test. (C) PAGE/western blotting analysis of AFP proteins in embryonic day 15.5 (E15.5), postnatal day 0.5 (P0.5), P7.5, and P14.5 WT, *Cbs*$^{+/-}$, and *Cbs*$^{-/-}$ mouse serum and liver (2.5 μg protein per lane). Postnatal repression of AFP expression was delayed in *Cbs*$^{-/-}$ mouse liver, and thus in *Cbs*$^{-/-}$ mouse serum.

surrounding non-cancer liver cells was found to be associated with high tumor stage and serum AFP level [24], and serum AFP elevation was found in NAFLD patients [25].

Previous studies demonstrated that human AFP contains a single glycosylation site but its structure varies with developmental stage and disease state, probably by alternating glycosylation

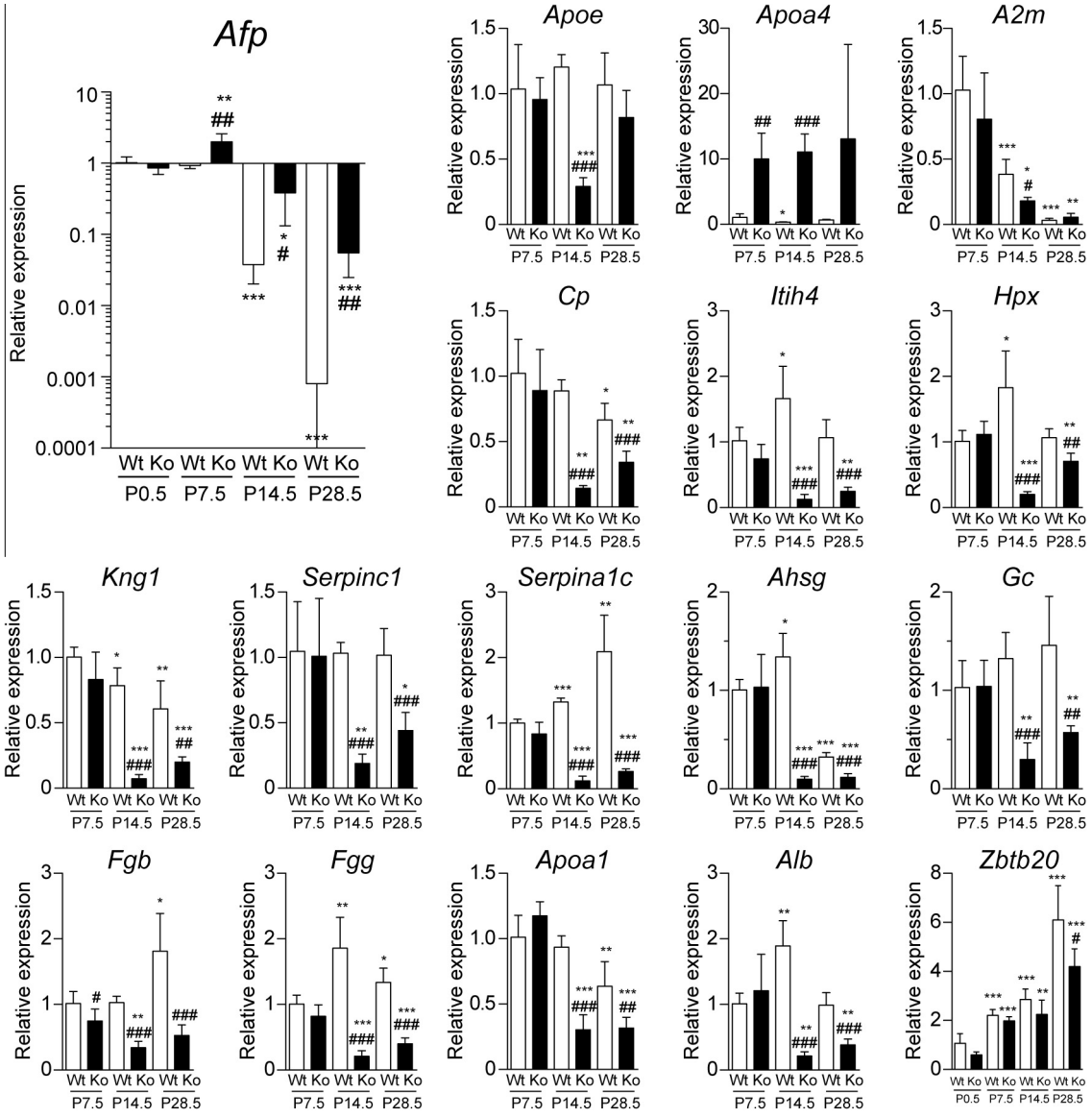

Fig. 3. Gene expression analysis of differentially expressed proteins and ZBTB20 in 2-week-old $Cbs^{-/-}$ mouse plasma by qPCR. Hepatic mRNA levels of α-fetoprotein (*Afp*), *apolipoprotein E* (*Apoe*), *apolipoprotein A-IV* (*Apoa4*), *α-2-macroglobulin* (*A2m*), *ceruloplasmin* (*Cp*), *inter α-trypsin inhibitor, heavy chain 4* (*itih4*), *hemopexin* (*Hpx*), *kininogen-1* (*Kng1*), *antithrombin-III* (*Serpinc1*), *α-1-antitrypsin 1-3* (*Serpina1c*), *α-2-HS-glycoprotein* (*Ahsg*), *vitamin D-binding protein* (*Gc*), *fibrinogen β chain* (*Fgb*), *fibrinogen γ chain* (*Fgg*), *apolipoprotein A-I* (*Apoa1*), *albumin* (*Alb*), and *Zbtb20* were analyzed by qPCR and normalized by *hypoxanthine guanine phosphoribosyl transferase* (*Hprt*) expression. The expression levels in wild-type mice (Wt) at postnatal day 0.5 (P0.5) (for *Afp* and *Zbtb20*) or P7.5 (for others) were set at 1. Data are shown as means ± SD ($n = 4–6$), and differences are significant in $^{*}P < 0.05$, $^{**}P < 0.01$ and $^{***}P < 0.001$ versus P0.5 (for *Afp* and *Zbtb*20) or P7.5 (for others); and $^{\#}P < 0.05$, $^{\#\#}P < 0.01$ and $^{\#\#\#}P < 0.001$ versus respective Wt samples by *t*-test.

status [26,27]. *Lens culinaris* agglutinin (LCA)-reactive fraction of AFP (AFP-L3) has been considered as a more specific HCC marker [27]. In this study, we detected hyperaccumulation of all nine AFP variants in 2-week-old $Cbs^{-/-}$ mouse plasma compared with respective wild-type samples (Fig. 2A), which was attributable to delayed repression of *Afp* expression in the liver (Fig. 2C). In contrast, expression of most other major plasma proteins was suppressed (Table 2 and Fig. 1A), at least partly, via transcriptional repression (Fig. 3). One plausible explanation is that increased AFP may bind and hold multiple endogenous ligands required for transcriptional activation of such liver proteins. This is because AFP belongs to a three-domain albuminoid gene family that currently consists of four members (AFP, albumin, vitamin D-binding protein, and α-albumin) and binds steroids, fatty acids, bilirubin, retinoids, and heavy metals [19,20]. Indeed, vitamin D-binding protein, which binds/transports vitamin D and plays important roles in bone/calcium homeostasis [28], was downregulated in 2-week-old $Cbs^{-/-}$ mouse plasma (Table 2 and Fig. 1A). This downregulation could be related to osteoporosis and skeletal abnormalities found in $Cbs^{-/-}$ mice [29], although transgenic mice overexpressing human AFP were found to be generally normal [30], and hereditary persistence of AFP in two unrelated Japanese families exhibited no apparent phenotypes [31]. We reported previously about abnormal and decreased high-density lipoprotein contents in 2-week-old $Cbs^{-/-}$ mouse serum [7], which may be associated with decreased apolipoprotein A-I levels (Table 2 and Fig. 1A).

In conclusion, we found transcriptionally regulated hyperaccumulation of AFP in fatty liver and plasma of juvenile $Cbs^{-/-}$ mice. Mice lacking methionine adenosyltransferase 1A also displayed

both fatty liver and AFP accumulation [32], but our *Cth*$^{-/-}$ mice did not [9]; therefore, the methionine cycle/transsulfuration pathway may play important roles in epigenetic regulation of *Afp*.

Conflict of interest

The authors declare no competing financial interests.

Acknowledgement

This work was supported by the Grants-in-Aid for Scientific Research (25460072 and 25220103) and the Program for Strategic Research Foundation at Private Universities (2011–2015) from the Ministry of Education, Culture, Sports, Science, and Technology (MEXT) of Japan; and Program for the Advancement of Next Generation Research and Keio Gijuku Fukuzawa Memorial Fund for the Advancement of Education and Research from the Keio University (to I.I.). S.K. is a research fellow of Japan Society for the Promotion of Science.

References

[1] Mudd, S.H., Levy, H.L. and Kraus, J.P. (2001) Disorders of transsulfuration in: The Metabolic and Molecular Basis of Inherited Disease (Scriver, C.R., Beaudet, W.S., Sly, W.S. and Valle, D., Eds.), 8th ed, pp. 2007–2056, MaGraw-Hill, New York.

[2] Austin, R.C., Lentz, S.R. and Werstuck, G.H. (2004) Role of hyperhomocysteinemia in endothelial dysfunction and atherothrombotic disease. Cell Death Differ. 11, S56–S64.

[3] Gaull, G., Sturman, J.A. and Schaffner, F. (1974) Homocystinuria due to cystathionine synthase deficiency: enzymatic and ultrastructural studies. J. Pediatr. 84, 381–390.

[4] Gulsen, M., Yesilova, Z., Bagci, S., Uygun, A., Ozcan, A., Ercin, C.N., Erdil, A., Sanisoglu, S.Y., Cakir, E., Ates, Y., Erbil, M.K., Karaeren, N. and Dagalp, K. (2005) Elevated plasma homocysteine concentrations as a predictor of steatohepatitis in patients with non-alcoholic fatty liver disease. J. Gastroenterol. Hepatol. 20, 1448–1455.

[5] Watanabe, M., Osada, J., Aratani, Y., Kluckman, K., Reddick, R., Malinow, M.R. and Maeda, N. (1995) Mice deficient in cystathionine beta-synthase: animal models for mild and severe homocyst(e)inemia. Proc. Natl. Acad. Sci. U.S.A. 92, 1585–1589.

[6] Ikeda, K., Kubo, A., Akahoshi, N., Yamada, H., Miura, N., Hishiki, T., Nagahata, Y., Matsuura, T., Suematsu, M., Taguchi, R. and Ishii, I. (2011) Triacylglycerol/phospholipid molecular species profiling of fatty livers and regenerated non-fatty livers in cystathionine beta-synthase-deficient mice, an animal model for homocysteinemia/homocystinuria. Anal. Bioanal. Chem. 400, 1853–1863.

[7] Namekata, K., Enokido, Y., Ishii, I., Nagai, Y., Harada, T. and Kimura, H. (2004) Abnormal lipid metabolism in cystathionine beta-synthase-deficient mice, an animal model for hyperhomocysteinemia. J. Biol. Chem. 279, 52961–52969.

[8] Akahoshi, N., Kobayashi, C., Ishizaki, Y., Izumi, T., Himi, T., Suematsu, M. and Ishii, I. (2008) Genetic background conversion ameliorates semi-lethality and permits behavioral analyses in cystathionine beta-synthase-deficient mice, an animal model for hyperhomocysteinemia. Hum. Mol. Genet. 17, 1994–2005.

[9] Ishii, I., Akahoshi, N., Yamada, H., Nakano, S., Izumi, T. and Suematsu, M. (2010) Cystathionine gamma-lyase-deficient mice require dietary cysteine to protect against acute lethal myopathy and oxidative injury. J. Biol. Chem. 285, 26358–26368.

[10] Yamada, H., Akahoshi, N., Kamata, S., Hagiya, Y., Hishiki, T., Nagahata, Y., Matsuura, T., Takano, N., Mori, M., Ishizaki, Y., Izumi, T., Kumagai, Y., Kasahara, T., Suematsu, M. and Ishii, I. (2012) Methionine excess in diet induces acute lethal hepatitis in mice lacking cystathionine gamma-lyase, an animal model of cystathioninuria. Free Radic. Biol. Med. 52, 1716–1726.

[11] Yamamoto, J., Kamata, S., Miura, A., Nagata, T., Kainuma, R. and Ishii, I. (2015) Differential adaptive responses to 1- or 2-day fasting in various mouse tissues revealed by quantitative PCR analysis. FEBS Open Bio 5, 357–368.

[12] Hagiya, Y., Kamata, S., Mitsuoka, S., Okada, N., Yoshida, S., Yamamoto, J., Ohkubo, R., Abiko, Y., Yamada, H., Akahoshi, N., Kasahara, T., Kumagai, Y. and Ishii, I. (2015) Hemizygosity of transsulfuration genes confers increased vulnerability against acetaminophen-induced hepatotoxicity in mice. Toxicol. Appl. Pharmacol. 282, 195–206.

[13] Xie, Z., Zhang, H., Tsai, W., Zhang, Y., Du, Y., Zhong, J., Szpirer, C., Zhu, M., Cao, X., Barton, M.C., Grusby, M.J. and Zhang, W.J. (2008) Zinc finger protein ZBTB20 is a key repressor of alpha-fetoprotein gene transcription in liver. Proc. Natl. Acad. Sci. U.S.A. 105, 10859–10864.

[14] Taketa, K. (1990) Alpha-fetoprotein: reevaluation in hepatology. Hepatology 12, 1420–1432.

[15] Masuzaki, R., Karp, S.J. and Omata, M. (2012) New serum markers of hepatocellular carcinoma. Semin. Oncol. 39, 434–439.

[16] Kajiyama, Y., Tian, J. and Locker, J. (2006) Characterization of distant enhancers and promoters in the albumin-alpha-fetoprotein locus during active and silenced expression. J. Biol. Chem. 281, 30122–30131.

[17] Spear, B.T. (1999) Alpha-fetoprotein gene regulation: lessons from transgenic mice. Semin. Cancer Biol. 9, 109–116.

[18] Terentiev, A.A. and Moldogazieva, N.T. (2013) Alpha-fetoprotein: a renaissance. Tumour Biol. 34, 2075–2091.

[19] Gillespie, J.R. and Uversky, V.N. (2000) Structure and function of alpha-fetoprotein: a biophysical overview. Biochim. Biophys. Acta 1480, 41–56.

[20] Mizejewski, G.J. (2004) Biological roles of alpha-fetoprotein during pregnancy and perinatal development. Exp. Biol. Med. (Maywood) 229, 439–463.

[21] Gabant, P., Forrester, L., Nichols, J., Van Reeth, T., De Mees, C., Pajack, B., Watt, A., Smitz, J., Alexandre, H., Szpirer, C. and Szpirer, J. (2002) Alpha-fetoprotein, the major fetal serum protein, is not essential for embryonic development but is required for female fertility. Proc. Natl. Acad. Sci. U.S.A. 99, 12865–12870.

[22] Bakker, J., De Mees, C., Douhard, Q., Balthazart, J., Gabant, P., Szpirer, J. and Szpirer, C. (2006) Alpha-fetoprotein protects the developing female mouse brain from masculinization and defeminization by estrogens. Nat. Neurosci. 9, 220–226.

[23] Akahoshi, N., Kamata, S., Kubota, M., Hishiki, T., Nagahata, Y., Matsuura, T., Yamazaki, C., Yoshida, Y., Yamada, H., Ishizaki, Y., Suematsu, M., Kasahara, T. and Ishii, I. (2014) Neutral aminoaciduria in cystathionine beta-synthase-deficient mice, an animal model of homocystinuria. Am. J. Physiol. Renal Physiol. 306, F1462–F1476.

[24] Kim, J., Hong, S.J., Park, J.H., Park, S.Y., Kim, S.W., Cho, E.Y., Do, I.G., Joh, J.W. and Kim, D.S. (2009) Expression of cystathionine beta-synthase is downregulated in hepatocellular carcinoma and associated with poor prognosis. Oncol. Rep. 21, 1449–1454.

[25] Babali, A., Cakal, E., Purnak, T., Biyikoglu, I., Cakal, B., Yuksel, O. and Koklu, S. (2009) Serum alpha-fetoprotein levels in liver steatosis. Hepatol. Int. 3, 551–555.

[26] Taketa, K., Sekiya, C., Namiki, M., Akamatsu, K., Ohta, Y., Endo, Y. and Kosaka, K. (1990) Lectin-reactive profiles of alpha-fetoprotein characterizing hepatocellular carcinoma and related conditions. Gastroenterology 99, 508–518.

[27] Nakagawa, T., Miyoshi, E., Yakushijin, T., Hiramatsu, N., Igura, T., Hayashi, N., Taniguchi, N. and Kondo, A. (2008) Glycomic analysis of alpha-fetoprotein L3 in hepatoma cell lines and hepatocellular carcinoma patients. J. Proteome Res. 7, 2222–2233.

[28] Gomme, P.T. and Bertolini, J. (2004) Therapeutic potential of vitamin D-binding protein. Trends Biotechnol. 22, 340–345.

[29] Liu, Y., Yang, R., Liu, X., Zhou, Y., Qu, C., Kikuiri, T., Wang, S., Zandi, E., Du, J., Ambudkar, I.S. and Shi, S. (2014) Hydrogen sulfide maintains mesenchymal stem cell function and bone homeostasis via regulation of Ca(2+) channel sulfhydration. Cell Stem Cell 15, 66–78.

[30] Yamashita, T., Kasai, N., Miyoshi, I., Sasaki, N., Maki, K., Sakai, M., Nishi, S. and Namioka, S. (1993) High level expression of human alpha-fetoprotein in transgenic mice. Biochem. Biophys. Res. Commun. 191, 715–720.

[31] Nagata-Tsubouchi, Y., Ido, A., Uto, H., Numata, M., Moriuchi, A., Kim, I., Hasuike, S., Nagata, K., Sekiya, T., Hayashi, K. and Tsubouchi, H. (2005) Molecular mechanisms of hereditary persistence of alpha-fetoprotein (AFP) in two Japanese families A hepatocyte nuclear factor-1 site mutation leads to induction of the AFP gene expression in adult livers. Hepatol. Res. 31, 79–87.

[32] Lu, S.C., Alvarez, L., Huang, Z.Z., Chen, L., An, W., Corrales, F.J., Avila, M.A., Kanel, G. and Mato, J.M. (2001) Methionine adenosyltransferase 1A knockout mice are predisposed to liver injury and exhibit increased expression of genes involved in proliferation. Proc. Natl. Acad. Sci. U.S.A. 98, 5560–5565.